Clusterin in Alzheimer's disease: an amyloidogenic inhibitor of amyloid formation

Panagiotis M. Spatharas[1], Georgia I. Nasi[1], Paraskevi L. Tsiolaki[1, †], Ioannis P. Trougakos[1], Vassiliki A. Iconomidou[1, *]

[1] Section of Cell Biology and Biophysics, Department of Biology, School of Sciences, National and Kapodistrian University of Athens, Panepistimiopolis, Athens 157 01, Greece

[†] Present Address: Department of Biochemistry and Biophysics, University of California, San Francisco, California 94143-2240, USA

[*] Corresponding author: veconom@biol.uoa.gr

e-mails:

Panagiotis M. Spatharas: panspatharas@biol.uoa.gr

Georgia I. Nasi: gnasi@biol.uoa.gr

Paraskevi L. Tsiolaki: etsiolaki@biol.uoa.gr

Ioannis P. Trougakos: itrougakos@biol.uoa.gr

Vassiliki A. Iconomidou: veconom@biol.uoa.gr

Total word count: 7,069 words (Including all 29 pages of text, figures, tables and respective legends)

Keywords: Clusterin, Molecular chaperones, Aggregation-prone regions, Amyloid, Amyloid-*β*, Amyloid inhibitors, Alzheimer's disease

Abstract

Clusterin is a heterodimeric glycoprotein (α- and β-chain), which has been described as an extracellular molecular chaperone. In humans, clusterin is an amyloid associated protein, co-localizing with fibrillar deposits in several amyloidoses, including Alzheimer's disease. To clarify its potential implication in amyloid formation, we located aggregation-prone regions within the sequence of clusterin α-chain, via computational methods. We had peptide-analogues of each region chemically synthesized and experimentally demonstrated that all of them can form amyloid-like fibrils. We also provide evidence that the same peptide-analogues can inhibit amyloid-β fibril formation. These findings elucidate parts of the molecular mechanism in which clusterin inhibits amyloid formation. At the same time, they hint that molecular chaperones with amyloidogenic properties might have a role in the regulation of amyloid formation, essentially acting as functional amyloids.

32 ## Introduction

33 Since the 17th century, physicians had already started to describe clinical disorders that were
34 later included in a broad group of diseases, nowadays known as amyloidoses (1). Prime
35 examples are Alzheimer's disease (AD), Parkinson's disease, type 2 diabetes and AL amyloidosis
36 (2). It is widely considered that these diseases are closely associated with the accumulation and
37 close packing of normally soluble proteins, which end up creating highly ordered, insoluble
38 aggregates. The so called amyloid fibrils, are deposited extracellularly in organs or tissues,
39 causing significant damage (2).

40 Molecular chaperones can inhibit amyloid formation in its early stages, thus preventing amyloid-
41 related cytotoxicity (3). Recent studies though, have shown that molecular chaperones can have
42 amyloidogenic properties (4-7), despite their seemingly contradicting physiological function. *In*
43 *vitro* experiments performed by our team have hinted that clusterin could be such a protein (7).
44 Clusterin is a ubiquitous, conserved mammalian glycoprotein, whose main isoform is secreted
45 and has been described as an extracellular molecular chaperone (8). Human clusterin precursor
46 is a 449 residue-long polypeptide chain, which, after having its signal peptide removed, is
47 reduced to 427 residues, and goes through several post-translational modifications (8). Mature
48 clusterin is cleaved in two chains —α-chain, consisting of 222 residues and β-chain, consisting of
49 205 residues— with five disulfide bonds forming between them (8). Its molecular weight is
50 approximately 80 kDa, almost 30% of it being carbohydrates, added by glycosylation (8).
51 Clusterin's structure has yet to be experimentally determined, but is believed to contain three
52 long molten globule-like regions and several amphipathic α-helices, which allow hydrophobic
53 interactions with its client-proteins (9).

54 Under normal circumstances, clusterin exists in solution as heterogeneous aggregates (10). It
55 has been suggested that, at mildly acidic pH (10), these aggregates disassociate and the
56 disassociated chaperone-active subunits function in an ATP-independent manner (11). They

57 bind misfolded client-proteins and form a high molecular weight complex. The formation of the
58 complex allows for stabilization of the misfolded proteins, which are consequently refolded by
59 other molecular chaperones (9) (visualized in Figure 1). Clusterin's ever-growing list of known
60 clients includes a variety of proteins, such as cellular receptors, apolipoproteins, the
61 complement complex, immunoglobulins, amyloid-forming proteins and non-protein molecules,
62 like lipids and heparin (12).

63 Having such a broad range of clients, it is only logical that clusterin contributes in many
64 physiological and pathological processes (13). AD is one of the most notable pathologies in
65 which clusterin is involved (12). Consistent with its chaperone function, clusterin keeps the
66 amyloid-*β* (A*β*) peptide soluble while transporting it in biological fluids, modulates its
67 permeation through the blood-brain barrier and contributes to its clearance, effectively halting
68 amyloid formation (14). In direct contradiction to that, it has been reported that clusterin
69 contributes to the early stages of AD pathogenesis (15, 16). To this day, clusterin's role in AD is
70 yet to be fully understood. Despite the mystery surrounding clusterin's implication in AD, it is a
71 known fact that it co-localizes with A*β* fibrillar deposits (12). This is also true for other
72 amyloidoses, in which clusterin is an amyloid associated protein (17).

73 It can be assumed that clusterin is found in the amyloid deposits because it is drifted along by its
74 client-proteins. In this study, we examined a different scenario, one that doesn't rule out the
75 possibility of clusterin being amyloidogenic itself. We used AMYLPRED (18), a consensus
76 algorithm for the prediction of amyloid propensity, in order to identify aggregation-prone
77 regions in clusterin *α*-chain. We had peptide-analogues of each region chemically synthesized
78 and experimentally demonstrated that all of them can form amyloid-like fibrils *in vitro*. The
79 same peptide-analogues, despite being amyloidogenic, can inhibit A*β* fibril formation. Based on
80 our findings, we proposed a putative mechanism in which clusterin prevents amyloid formation.
81 The suggested mechanism could also explain the contradictory reports that hint at clusterin's
82 implication in the acceleration of the appearance of AD symptoms. At the same time, we hope

83 that the basis of clusterin's amyloid inhibiting activity could give insight into the implementation
84 of peptide-based amyloidogenesis inhibitors in the treatment of amyloidoses.

85 Results & Discussion

86 All wild-type clusterin *α*-chain peptide-analogues form amyloid-like fibrils *in vitro*

87 According to the prediction of AMYLPRED, clusterin *α*-chain has five aggregation-prone regions.
88 The peptide-analogues that correspond to those regions are NFHAMFQ, AMDIHF, ILSVD,
89 YYLRVTT and EVVVKLF, as depicted in Figure 2. NFHAMFQ has previously been studied by our
90 lab and proved to exhibit amyloidogenic properties *in vitro* (7). Our current findings reveal that
91 AMDIHF, ILSVD, YYLRVTT, and EVVVKLF can also be characterized as amyloidogenic *in vitro*,
92 making a total of five experimentally verified aggregation-prone regions in clusterin *α*-chain.
93 Characterization was based on the tinctorial criteria, which are commonly used for the
94 identification of amyloid fibrils (transmission electron microscopy, X-ray diffraction from protein
95 fibers, ATR FT-IR spectroscopy and Congo Red birefringence assay) (19).

96 Transmission electron micrographs show that AMDIHF, ILSVD, YYLRVTT, and EVVVKLF self-
97 assemble into amyloid-like fibrils (Figure 3 a-d, respectively). AMDIHF fibrils exhibit
98 considerable polymorphism, forming both supercoils and tapes (Figure 3a, red and blue arrows,
99 respectively), while EVVVKLF fibrils form very wide and prominent tapes (Figure 3d, blue arrow).
100 ILSVD forms amyloid-like fibrils that are packed more densely when compared to the other
101 peptides (Figure 3b), indicating that it could be the most aggregation-prone region in clusterin
102 α-chain.

103 Oriented fibers formed by each peptide solution, produce X-ray diffraction patterns, indicative
104 of the presence of the "cross-*β*" structure. Most reflections are ring-like, most likely because
105 the fibrils are not perfectly aligned in a parallel manner (20). The exact measurements for each
106 of the four diffraction patterns can be seen in Figure 3 (e-h). It is worth pointing out, that
107 EVVVKLF diffraction pattern has two equatorial reflections. This could be due to the *β*-sheets

108 being antiparallel and each *β*-strand having residues with a considerable difference in side-chain
109 length at each side. The dominance of the *β*-sheet secondary structure is supported by ATR FT-
110 IR spectroscopy data, since the spectra of all the peptide-analogues reveal bands that can be
111 assigned to *β*-sheets (21) (Table 1 and Figure 3 m-o).

112 Every peptide binds Congo Red, as seen under bright field illumination in a polarizing
113 stereomicroscope (Figure 3 i-l, upper). When the polars are crossed, the peptides exhibit the
114 apple-green birefringence (Figure 3 i-l, lower) that amyloids typically exhibit.

115 **Full-length clusterin could also have amyloidogenic properties**

116 Recent studies have shown that short aggregation-prone segments, known as amyloidogenic
117 determinants, can lead to amyloid formation, even when they are inserted in non-
118 amyloidogenic proteins, via protein engineering (22). The fact that clusterin has five such
119 segments in its *α*-chain, provides potent indication that the *α*-chain and consequently the full-
120 length protein, may intrinsically exhibit amyloidogenicity. This argument has fascinating
121 implications, especially considering clusterin's role as a molecular chaperone.

122 **Molecular chaperones and their involvement in amyloid formation and inhibition**

123 One of the fundamental functions of molecular chaperones is considered to be the prevention
124 of protein aggregation and consequently, amyloid fibril formation (3). Based on that notion, it
125 has been suggested that molecular chaperones could be used as anti-amyloid drugs (23). In
126 direct contradiction to that, clusterin has the potential to form amyloid-like fibrils. In fact, there
127 have been reports of other proteins that function as molecular chaperones and exhibit
128 amyloidogenicity *in vitro* (5, 6) or *in vivo* (4). Despite lacking any sequence similarity, this group
129 of proteins shares a significant number of similar features, besides having the potential to form
130 amyloid-like fibrils.

131 A prominent example is *α*-crystallin, a small heat shock protein (sHSP), which is highly expressed
132 in the eye lens. Full-length *α*-crystallin has been found to form amyloid-like fibrils *in vitro*(5) and

133 is believed to be implicated in the formation of cataract (24). As most sHSPs, *α*-crystallin
134 exhibits remarkable structural plasticity, which is intertwined with its chaperone activity (25).
135 Interestingly, *α*-crystallin's chaperone activity is exhibited in a very similar manner to that of
136 clusterin (26). sHSPs exist in solution as oligomeric structures, ranging from 9 to 50 subunits.
137 Those structures disassociate under stress and release functional subunits (27). *α*-crystallin in
138 particular, possesses a dynamic oligomeric structure, which, under increasing temperature,
139 allows exchange of subunits within proximate oligomers. The so-called "traveling subunits" are
140 believed to play a fundamental role in *α*-crystallin's chaperone activity, by exposing hydrophobic
141 surfaces and consequently, allowing hydrophobic interactions with misfolded proteins, including
142 A*β* (28-30). Even though this is the physiological mechanism in which *α*-crystallin functions, it is
143 reminiscent of how amyloidogenic proteins behave on their way to self-assembly and formation
144 of amyloid fibrils (31). This might explain the reports of *α*-crystallin forming amyloid-like fibrils
145 *in vitro (5)*.

146 Another relevant example is that of the caseins, a group of proteins that comprise the largest
147 part of the total protein content in milk (32) and are usually found in aggregates, known as
148 casein micelles. The micelles are primarily composed of four major proteins, namely α_{s1}-, α_{s2}-, *β*-
149 and *κ*-casein (33). All four of them have been classified as intrinsically disordered proteins,
150 because of the considerable structural flexibility that they exhibit (34). In consistence with
151 clusterin and *α*-crystallin, the major casein proteins are believed to function as molecular
152 chaperones (35), while *κ*-casein forms amyloid fibrils *in vitro* (6) and α_{s2}-casein forms amyloid
153 fibrils *in vivo*, in corpora amylacea in the bovine mammary gland (2, 4). Yet, in physiological
154 conditions, α_{s1}-casein interacts with α_{s2}-casein, forming α_{s}-casein, effectively halting the
155 formation of amyloid fibrils (36). Similarly, α_{s}-casein and *β*-casein inhibit *κ*-casein amyloid
156 formation, by shielding monomeric *κ*-casein hydrophobic surfaces with similar regions of their
157 respective sequences (37).

158 In summary, clusterin, *α*-crystallin, and the casein proteins share common features:

159 (1) They function as molecular chaperones, by exposing hydrophobic regions, interacting with and
160 stabilizing misfolded proteins on their way to aggregation (9, 11, 28, 29, 35-38).
161 (2) They show structural plasticity, either having molten globule-like or intrinsically disordered
162 regions on their sequence (11, 25, 34).
163 (3) They are found in solution as heterogeneous aggregates, oligomers or micelles, which
164 dissociate under conditions of stress (10, 27, 33).
165 (4) They all interact with one, or more amyloidogenic proteins (7, 12, 30, 36, 37).
166 (5) Parts of their sequence, or the full-length proteins, are known to form amyloid-like fibrils *in*
167 *vitro* or *in vivo* (4-7).

168 These similarities may underlie a common mechanism in which the cell prevents toxic amyloid
169 formation under different conditions of stress, by utilizing the intrinsic amyloidogenicity of
170 specific molecular chaperones. For clusterin, amyloidogenesis inhibition could be activated
171 under pH-induced stress and achieved through the interaction of its aggregation-prone regions
172 with amyloidogenic proteins, on their way to aggregation. Likewise, *α*-crystallin could act under
173 temperature-induced stress and the casein proteins may present a more specific system of
174 amyloid inhibition, present primarily at the mammary gland.

175 **Clusterin *α*-chain peptide-analogues inhibit A*β*$_{42}$ amyloid formation *in vitro***

176 To reinforce the claim that clusterin mediates amyloidogenesis inhibition, via its aggregation-
177 prone regions, we investigated the *in vitro* effects of the clusterin *α*-chain peptide-analogues on
178 A*β*$_{42}$ fibril formation. Each clusterin peptide was co-incubated with equimolar amounts of A*β*$_{42}$
179 and the aggregation kinetics were evaluated with Thioflavin T fluorescence measurements over
180 time and transmission electron microscopy (TEM) imaging. It is important to note that, full-
181 length clusterin is known to inhibit A*β* fibril formation *in vitro (39)*, thus, our purpose is to
182 pinpoint segments of its sequence that could as catalysts for said inhibition.

183 ThT fluorescent measurements reveal that individual Aβ_{42} starts forming fibrils almost
184 immediately and reaches maximal fluorescence signal after approximately 7 hours. When co-
185 incubated with the clusterin peptide-analogues (Aβ_{42}+NFHAMFQ, Aβ_{42}+AMDIHF, Aβ_{42}+ILSVD,
186 Aβ_{42}+YYLRVTT, and Aβ_{42}+EVVVKLF), Aβ_{42} exhibits decreased emission. ILSVD and especially
187 EVVVKLF seem to be the most potent inhibitors (Figure 4j and 4p, respectively). As previously
188 shown, individual ILSVD is incredibly amyloidogenic, as is Aβ_{42}. The fact that interaction
189 between the two leads to decreased fibril formation, hints that peptides with high
190 amyloidogenic potential, could negate each other's fibril-forming properties. EVVVKLF bears
191 some sequence similarity with ^{16}KLVFFA^{21}, a key amyloid-forming segments of Aβ_{42} (40).
192 Considering that peptide-analogues derived from ^{16}KLVFFA^{21} have been suggested as potential
193 therapeutic agents for the treatment of AD (41), it is not surprising that EVVVKLF has the highest
194 inhibiting effect among the five peptides. NFHAMFQ and AMDIHF also seem to inhibit Aβ_{42} fibril
195 formation (Figure 4f and 4h, respectively), but their potential as inhibitors is less significant than
196 that of ILSVD and EVVVKLF. YYLRVTT effectively delays fibril formation, but after approximately
197 20 hours, fluorescence signal begins to rise (Figure 4n). After 40 hours, Aβ_{42}+YYLRVTT reaches
198 fluorescence intensity levels which are comparable to those of individual Aβ_{42}.

199 TEM confirms that all five peptide-analogues inhibit or delay Aβ_{42} amyloid formation, after 7
200 days of incubation. When individually incubated, Aβ_{42} forms straight and unbranched fibrils
201 with indefinite length and a diameter of approximately 80 Å (Figure 4 b-d). A small number of
202 fibrils is observed after 1 day of incubation (Figure 4b). The population of fibrils increases
203 significantly after 3 days (Figure 4c) and reaches its maximum after 7 days (Figure 4d). As
204 expected, ILSVD and EVVVKLF prove to be the most potent inhibitors (Figure 4i and 4o,
205 respectively). The entire grids were thoroughly examined, and no fibrils were observed.
206 NFHAMFQ and AMDIHF also inhibit Aβ_{42} fibril formation, as fibrils were not observed anywhere
207 on the grid (Figure 4e and 4g, respectively). However, both seem to induce the formation of
208 amorphous aggregates. AMDIHF seems to delay, but not inhibit fibril formation. In contrast to

209 the other peptides, fibrils can be observed (Figure 4m). The number of fibrils is similar to that of
210 individual Aβ_{42}, after 1 day of incubation. Much like NFHAMFQ and AMDIHF, YYLRVTT also
211 seems to induce the formation of amorphous aggregates.

212 **A putative mechanism for clusterin-mediated inhibition of A*β* amyloidogenesis**

213 Having established that clusterin *α*-chain peptide analogues can inhibit A*β* amyloidogenesis *in*
214 *vitro*, we opted to propose a mechanism in which clusterin could use its aggregation-prone
215 regions to exert its molecular chaperone activity on A*β*.

216 It is believed that A*β* amyloidogenesis is promoted by acidic pH (42). As previously mentioned,
217 mildly acidic pH also allows the disassociation of clusterin's heterogeneous aggregates, releasing
218 chaperone-active subunits (10). In its disassociated form, clusterin is assumed to
219 hydrophobically interact with its client-proteins through amphipathic *α*-helices, which are
220 surrounded by molten globule-like regions (9). ^{12}NFHAMFQ^{18}, one of clusterin's aggregation-
221 prone regions, is located on a putative amphipathic *α*-helix. However, we have already proved
222 that NFHAMFQ also has the propensity to form *β*-strands (7), hinting that the broader region has
223 the intrinsic conformational properties of a chameleon sequence. When in proximity with an A*β*
224 fibril, the *α*-helical ^{12}NFHAMFQ^{18} could unfold and then refold into a *β*-strand, allowing
225 interaction with A*β*'s *β*-stranded regions and temporarily halting fibril growth. This process
226 could trigger the exposition of clusterin's other aggregation-prone regions and allow it to attach
227 itself at the edge of the A*β* fibril, via *β*-strand hydrogen bonding. In this manner, it would not
228 allow A*β* monomers to elongate the fibril, effectively blocking further polymerization. At the
229 same time, free clusterin subunits could bind to A*β* monomers, forming complexes and
230 stabilizing their structure, until it passes the baton to other molecular chaperones, once again,
231 halting fiber growth and minimizing the possibility of toxic secondary nucleation (43). The
232 suggested mechanism is visualized in Figure 5.

233 The putative mechanism that was just described, is also supported by recent studies, which have
234 identified a novel, pathological mutation on clusterin's gene, in AD patients. In particular,
235 p.I360N changes the aggregation-prone region ^{81}ILSVD^{85} to ^{81}NLSVD^{85} (44). The resulting
236 sequence is not predicted by AMYLPRED, hinting that it is not aggregation-prone anymore. To
237 experimentally confirm that the mutated region is not aggregation-prone, we had NLSVD
238 chemically synthesized. Indeed, TEM shows that NLSVD does no longer self-assemble into
239 amyloid fibrils (data not shown). Also, NLSVD does not form oriented fibers, suitable for X-ray
240 diffraction, hinting that there are no fibrils in its solution. Finally, when stained with Congo Red
241 and stereoscopically observed between crossed polars, it does not exhibit apple-green
242 birefringence (data not shown). Considering that out of the peptides we examined, ILSVD is
243 hinted to be one of the better A*β* fibril formation inhibitors, this mutation could lead to a
244 malfunction in the clusterin-mediated amyloidogenesis inhibition system. Thus, the
245 pathogenicity of the phenotype could be explained by clusterin's inability to inhibit amyloid
246 formation, due to the absence of its most aggregation-prone region, that being ^{81}ILSVD^{85}, which
247 would normally act as a breaker to A*β* fibril elongation. As expected, ThT kinetics and TEM
248 imaging show that NLSVD does not inhibit Aβ_{42} amyloid formation *in vitro*. Aβ_{42} and Aβ_{42}+NLSVD
249 fluorescence curves mostly overlap, while Aβ_{42}+NLSVD show a slightly enhanced fluorescence
250 peak (Figure 4k). Transmission electron micrographs reveal that Aβ_{42} fibril morphology is vastly
251 different to that of Aβ_{42}+NLSVD. Aβ_{42}+NLSVD fibrils after 7 days of incubation, are wider, not as
252 linear and are more densely packed, than those of Aβ_{42}, after the same incubation period
253 (Figure 4l). Furthermore, Aβ_{42}+NLSVD fibrils interact with each other and create bulky
254 structures, which are not formed by individual Aβ_{42}.

255 The aforementioned mechanism can explain why clusterin is found co-localized with the A*β*
256 fibrillar deposits (12) and is consistent with reports of clusterin decelerating A*β* fibril formation
257 (43, 45). However, clusterin's occasional contribution to the appearance of AD symptoms (15,
258 16) needs further elucidation. It is logical to assume that, when A*β* misfolded monomers are

259 produced faster than what clusterin's existing population can process, the resulting complexes
260 would fail to stabilize A*β*'s structure, essentially bringing remote misfolded monomers into
261 proximity. This could accelerate amyloid fibril formation (Figure 5), while clusterin would end
262 up co-localized with the fibrillar deposits. This hypothesis is supported by the findings of
263 Yerbury *et al*., which show that clusterin's enhancing effect on amyloid formation is caused by
264 low clusterin:substrate ratio (39). A relevant example could be found in patients with familial
265 Alzheimer's disease (FAD), where A*β* is produced much faster than usual (46). In fact, most pre-
266 clinical studies on AD use FAD animals as models, because it is a guaranteed method of
267 acquiring early-onset AD test subjects (47). This could also be the case for Oh *et. al*, who
268 showed that clusterin-null 5XFAD mice, show AD symptoms later than their littermate
269 counterparts (15). In the end, molecular chaperone-mediated amyloidogenesis inhibition,
270 seems to be a double-edged sword for the cell, effective, but at the same time, conditionally
271 harmful. The inadvertent bias that pre-clinical studies introduce, using test subjects with FAD,
272 rather than sporadic AD, could make the inhibition system seem much more flawed than it
273 really is.

274 **Peptide-based amyloidogenesis inhibitors, derived from aggregation-prone protein regions**

275 We ultimately proposed that the cell can prevent amyloid formation by utilizing the intrinsic
276 amyloidogenicity of specific molecular chaperones, similar to how functional amyloids work. If
277 that statement proves to be true, harnessing the ability of molecular chaperones to halt amyloid
278 formation could be essential to tackling AD and other amyloidoses. The key to inhibiting
279 amyloid formation lies in the aggregation-prone regions of said proteins, thus synthesizing and
280 studying peptides from such regions could provide novel inhibitors of A*β* amyloidogenesis and
281 amyloid formation in general (48).

282 It is worth mentioning that, the ability of molecular chaperones to inhibit amyloid formation
283 doesn't seem to be substrate-specific, meaning that one chaperone could act as an
284 amyloidogenesis inhibitor for a variety of different amyloidogenic proteins, even if they are not

285 known to interact *in vivo*. For example, though *α*-crystallin is known to interact with A*β* (30), the
286 casein proteins are not. Despite that, all of them can inhibit A*β* amyloidogenesis *in vitro (49,*
287 *50)*. Furthermore, this also seems to be the case for aggregation-prone peptides that are not
288 derived from regions of molecular chaperones (40). Mimicking the physiological system for
289 amyloidogenesis prevention and extending it to aggregation-prone peptide-analogues of non-
290 chaperone-active proteins could provide us with a much greater variety of potential inhibitors.

291 Despite the potential that specific peptides show as amyloidogenesis inhibitors, it is of vital
292 importance to ensure that they are non-toxic for the cell. It is noteworthy that, even though
293 some molecular chaperones have amyloidogenic properties, they seem to not have negative
294 effects on the survival of the cell. In a similar manner, functional amyloids are not harmful to
295 the organisms in which they appear. It is believed that controlling the expression of
296 amyloidogenic proteins, regulating fibril formation with co-localized proteins-molecules and the
297 fact that they are often found isolated inside membrane bound compartments, are some of the
298 reasons why functional amyloids are not toxic (51). For the peptide-inhibitors to be usable,
299 these questions must be accurately answered, and the findings should be incorporated in their
300 implementation as potential drugs for amyloidoses, especially when it comes to peptide
301 concentration and the complementary substances that should be administered.

302 Materials and Methods

303 Prediction of potential aggregation-prone regions in human clusterin

304 AMYLPRED(18), a consensus algorithm for the prediction of amyloid propensity, was used for
305 the identification of aggregation-prone regions in wild-type, mature clusterin (Uniprot AC:
306 P10909). The *α*-chain, which is our focus in the current study, has five such regions. The first
307 one (^{12}NFHAMFQ^{18}) has previously been studied by our lab and proved to exhibit amyloidogenic
308 properties *in vitro* (7). This time, we opted to study the remaining four, those being ^{31}MDIHF^{35},
309 ^{82}LSV^{84}, ^{155}YYLRVTT^{161} and ^{177}EVVVKLF^{183}.

310 **Peptide synthesis**

311 All peptide-analogues were synthesized and lyophilized by GeneCust© Europe, France. The
312 exact sequences for the peptide-analogues were NFHAMFQ, AMDIHF, ILSVD, NLSVD, YYLRVTT
313 and EVVVKLF. The regions that were used for the second and third peptide-analogues were
314 ^{30}AMDIHF^{35} and ^{81}ILSVD^{85}, which are extensions of the original predicted regions. NLSVD is a
315 mutant counterpart of ILSVD. The purity of all the synthesized peptides was higher than 98%,
316 with the N- and C-terminals being free.

317 Aβ_{42} was also synthesized and lyophilized by GeneCust© Europe, France. The exact sequence is
318 DAEFRHDSGYEVHHQKLVFFAEDVGSNKGAIIGLMVGGVVIA. The purity of the peptide was higher
319 than 95%, with the N- and C-terminals being free.

320 **Sample preparation**

321 **Disaggregation of pre-existing aggregates:** Each lyophilized peptide was dissolved in
322 1,1,1,3,3,3-Hexafluoro-2-propanol (HFIP; Sigma©) at a concentration of 1 mg/mL. All clusterin
323 peptides were mixed with equimolar amounts of Aβ_{42}. Individual peptide solutions and Aβ_{42}-
324 clusterin peptide solutions were left to dry overnight in a fume hood, at room temperature, until
325 thin peptide-containing films were created. The peptide-containing films were stored at -20 °C.

326 ***In vitro* fibril formation:** The peptide-containing films were left at room temperature for 30
327 minutes and dissolved in 0.1 M HEPES buffer (pH=7.4; Sigma©) or dH_2O (pH=5.57), at
328 concentrations ranging from 10 µM to 1 mM. The peptide solutions were incubated for 1 week
329 at 37 °C, unless stated otherwise.

330 **Transmission Electron Microscopy (TEM).**

331 A 3 µL droplet of 100 µM peptide solution was applied to glow-discharged 400-mesh carbon-
332 coated copper grids for 60 seconds. Directly afterwards, the grids were stained with a 3 µL
333 droplet of 2% (w/v) aqueous uranyl acetate for another 60 seconds. Excess stain was blotted
334 away with filter paper and air-dried. The grids were examined with a Morgagni™ 268

335 transmission electron microscope, operated at 80 kV. Digital acquisitions were performed with
336 an 11 Mpixel side mounted Morada CCD camera (Soft Imaging System, Muenster, Germany).

337 **X-ray diffraction from oriented protein fibers.**

338 **Oriented fiber formation:** 1 mM aqueous peptide solutions were incubated for two weeks, to
339 form viscous solutions, which facilitate the formation of oriented fibers. A 10 µL droplet of each
340 peptide solution was placed between two quartz capillaries covered with wax, spaced
341 approximately 1.5 mm apart and mounted horizontally on a glass substrate, as collinearly as
342 possible. The droplet was allowed to dry for 3 days, until oriented fibers were formed.

343 **X-ray diffraction and analysis:** The oriented fibers were shot with X-rays and diffracted. The X-
344 ray diffraction pattern was collected using a SuperNova-Agilent Technologies X-ray generator,
345 equipped with a 135 mm ATLAS CCD detector and a 4-circle kappa goniometer, at the Institute
346 of Biology, Medicinal Chemistry and Biotechnology, National Hellenic Research Foundation
347 (CuKα high intensity X-ray micro-focus source, λ = 1.5418 Å), operated at 50 kV, 0.8 mA. The
348 specimen-to-film distance was set at 52mm and the exposure time was set to 200s. The X-ray
349 patterns were initially viewed using CrysAlisPro (52) and afterwards measured with iMosFLM
350 (53).

351 **Attenuated total reflectance Fourier-transform infrared (ATR FT-IR) spectroscopy.**

352 A 10 µL droplet of 1 mM aqueous peptide solution was cast on a front-coated Au mirror and left
353 to dry slowly at room temperature, until a thin peptide-containing film was created. Infrared
354 spectra were obtained from these films at a resolution of 4 cm^{-1}, utilizing an IR microscope
355 (IRScope II by Bruker Optics) equipped with a Ge attenuated total reflectance (ATR) objective
356 lens (20x) and attached to a Fourier-transform infrared (FT-IR) spectrometer (Equinox 55, by
357 Bruker Optics). Ten 32-scan spectra were collected from each sample and averaged to improve
358 the sound/noise (S/N) ratio. Both are shown in the absorption mode after correction for the
359 wavelength dependence of the penetration depth (pd-λ). Absorption band maxima were

360 determined from the minima in the second derivative of the corresponding spectra. Derivatives
361 were computed analytically using routines of the Bruker OPUS/OS2 software, including
362 smoothing over a ±13 cm^{-1} range around each data point, performed by the Savitzky–Golay (54)
363 algorithm. Data was visualized using OriginPro 7. Individual clusterin peptide solutions were
364 also examined at a concentration of 500 µM.

365 **Congo Red Birefringence Assay.**

366 A 3 µL droplet of 500 µM peptide solution was applied to glass slides and stained with a 10 mM
367 Congo Red (Sigma©) solution in PBS (137 mM NaCl, 27 mM KCl, 100 mM Na_2HPO_4, 18 mM
368 KH_2PO_4, pH=7.4) or dH_2O for approximately 30 minutes. Then, they were washed several times
369 with 90% ethanol and were left to dry approximately for 10 minutes. The samples were
370 observed under bright field illumination and between crossed polars, using a Leica MZ7.5
371 polarizing stereomicroscope, equipped with a Sony *α*6000 camera.

372 **Thioflavin T (ThT) Kinetic Assay**

373 ThT fluorescence measurements were conducted at 37 °C, in black 96-well plates with flat, clear
374 bottoms, using a Tecan Spark microplate reader. The top of the plates was sealed with
375 microplate covers and the fluorescence readings were performed through the bottom. A 444
376 nm filter was used for excitation and a 484 nm filter for emission. The reaction solutions
377 contained freshly prepared 10 µM disaggregated peptide solutions (individual Aβ_{42} or Aβ_{42}-
378 clusterin peptide solutions) and 25 µM ThT (Sigma©) in dH_2O. ThT fluorescence was also
379 measured in the absence of peptide solutions. Each experiment was conducted in triplicates.
380 Measurement lasted for 50 hours and fluorescence readings were collected every 15 minutes.
381 ThT background fluorescence was subtracted from the peptide fluorescence readings at each
382 time point. Standard deviation was calculated, and the data was normalized. 100 arbitrary units
383 correspond to maximum individual Aβ_{42} fluorescence intensity. Data was visualized using
384 RStudio (package ggplot2).

Acknowledgments

This research has been co-financed by the European Union and Greek national funds through the Operational Program "Competitiveness, Entrepreneurship and Innovation", under the call "RESEARCH – CREATE – INNOVATE" (project code: T1EDK-00353). We acknowledge support of this work by the project “INSPIRED-The National Research Infrastructures on Integrated Structural Biology, Drug Screening Efforts and Drug target functional characterization” (MIS 5002550) which is implemented under the Action “Reinforcement of the Research and Innovation Infrastructure”, funded by the Operational Program “Competitiveness, Entrepreneurship and Innovation” (NSRF 2014-2020) and co-funded by Greece and the European Union (European Regional Development Fund). We also acknowledge Dr. George Baltatzis for kindly assisting us with handling the Morgagni Microscope at the 1st Department of Pathology, Medical School, National and Kapodistrian University of Athens. Finally, we acknowledge the support of Dr. Aimilia Sklirou, who kindly assisted with handling the Tecan Spark microplate reader.

Author contributions

P.M.S. performed sample preparation, Congo Red birefringence and ThT kinetics assays, acquired and processed TEM, X-ray diffraction and ATR FT-IR spectroscopy data, helped in conceiving the project and wrote the initial draft of the manuscript. G.I.N. participated and assisted in all the experiments. P.L.T co-supervised and helped in conceiving the project. I.P.T. helped in conceiving the project and supervised the ThT kinetics assays. V.A.I. supervised and helped in conceiving the project. All authors discussed the results and edited or commented on the manuscript.

Conflict of interest

The authors declare no conflicts of interest.

409 **References**

410 1. Kyle RA. Amyloidosis: a brief history. Amyloid : the international journal of experimental
411 and clinical investigation : the official journal of the International Society of Amyloidosis.
412 2011;18 Suppl 1:6-7.

413 2. Benson MD, Buxbaum JN, Eisenberg DS, Merlini G, Saraiva MJM, Sekijima Y, et al.
414 Amyloid nomenclature 2020: update and recommendations by the International Society of
415 Amyloidosis (ISA) nomenclature committee. Amyloid : the international journal of experimental
416 and clinical investigation : the official journal of the International Society of Amyloidosis.
417 2020;27(4):217-22.

418 3. Wentink A, Nussbaum-Krammer C, Bukau B. Modulation of Amyloid States by Molecular
419 Chaperones. Cold Spring Harbor perspectives in biology. 2019.

420 4. Niewold TA, Murphy CL, Hulskamp-Koch CA, Tooten PC, Gruys E. Casein related amyloid,
421 characterization of a new and unique amyloid protein isolated from bovine corpora amylacea.
422 Amyloid : the international journal of experimental and clinical investigation : the official journal
423 of the International Society of Amyloidosis. 1999;6(4):244-9.

424 5. Ecroyd H, Carver JA. Crystallin proteins and amyloid fibrils. Cellular and molecular life
425 sciences : CMLS. 2009;66(1):62-81.

426 6. Ecroyd H, Thorn DC, Liu Y, Carver JA. The dissociated form of kappa-casein is the
427 precursor to its amyloid fibril formation. The Biochemical journal. 2010;429(2):251-60.

428 7. Tsiolaki PL, Nastou KC, Louros NN, Hamodrakas SJ, Iconomidou VA. Exploring
429 Amyloidogenicity of Clusterin: A Structural and Bioinformatics Analysis. Advances in
430 experimental medicine and biology. 2017;989:93-107.

431 8. Jones SE, Jomary C. Clusterin. The international journal of biochemistry & cell biology.
432 2002;34(5):427-31.

433 9. Bailey RW, Dunker AK, Brown CJ, Garner EC, Griswold MD. Clusterin, a binding protein
434 with a molten globule-like region. Biochemistry. 2001;40(39):11828-40.

435 10. Poon S, Rybchyn MS, Easterbrook-Smith SB, Carver JA, Pankhurst GJ, Wilson MR. Mildly
436 acidic pH activates the extracellular molecular chaperone clusterin. The Journal of biological
437 chemistry. 2002;277(42):39532-40.
438 11. Poon S, Easterbrook-Smith SB, Rybchyn MS, Carver JA, Wilson MR. Clusterin is an ATP-
439 independent chaperone with very broad substrate specificity that stabilizes stressed proteins in
440 a folding-competent state. Biochemistry. 2000;39(51):15953-60.
441 12. Calero M, Rostagno A, Frangione B, Ghiso J. Clusterin and Alzheimer's disease. Sub-
442 cellular biochemistry. 2005;38:273-98.
443 13. Rohne P, Prochnow H, Koch-Brandt C. The CLU-files: disentanglement of a mystery.
444 Biomolecular concepts. 2016;7(1):1-15.
445 14. Matsubara E, Soto C, Governale S, Frangione B, Ghiso J. Apolipoprotein J and
446 Alzheimer's amyloid beta solubility. The Biochemical journal. 1996;316 (Pt 2):671-9.
447 15. Oh SB, Kim MS, Park S, Son H, Kim SY, Kim MS, et al. Clusterin contributes to early stage
448 of Alzheimer's disease pathogenesis. Brain pathology. 2019;29(2):217-31.
449 16. DeMattos RB, O'Dell M A, Parsadanian M, Taylor JW, Harmony JA, Bales KR, et al.
450 Clusterin promotes amyloid plaque formation and is critical for neuritic toxicity in a mouse
451 model of Alzheimer's disease. Proceedings of the National Academy of Sciences of the United
452 States of America. 2002;99(16):10843-8.
453 17. Nastou KC, Nasi GI, Tsiolaki PL, Litou ZI, Iconomidou VA. AmyCo: the amyloidoses
454 collection. Amyloid : the international journal of experimental and clinical investigation : the
455 official journal of the International Society of Amyloidosis. 2019;26(3):112-7.
456 18. Frousios KK, Iconomidou VA, Karletidi CM, Hamodrakas SJ. Amyloidogenic determinants
457 are usually not buried. BMC structural biology. 2009;9:44.
458 19. Sunde M, Blake CC. From the globular to the fibrous state: protein structure and
459 structural conversion in amyloid formation. Quarterly reviews of biophysics. 1998;31(1):1-39.

460 20. Makin OS, Serpell LC. X-ray diffraction studies of amyloid structure. Methods in
461 molecular biology. 2005;299:67-80.
462 21. Surewicz WK, Mantsch HH, Chapman D. Determination of protein secondary structure
463 by Fourier transform infrared spectroscopy: a critical assessment. Biochemistry. 1993;32(2):389-
464 94.
465 22. Teng PK, Eisenberg D. Short protein segments can drive a non-fibrillizing protein into the
466 amyloid state. Protein engineering, design & selection : PEDS. 2009;22(8):531-6.
467 23. Yerbury JJ, Kumita JR. Protein chemistry of amyloid fibrils and chaperones: implications
468 for amyloid formation and disease. Current Chemical Biology. 2010;4(2):89-98.
469 24. Meehan S, Berry Y, Luisi B, Dobson CM, Carver JA, MacPhee CE. Amyloid fibril formation
470 by lens crystallin proteins and its implications for cataract formation. The Journal of biological
471 chemistry. 2004;279(5):3413-9.
472 25. Basha E, O'Neill H, Vierling E. Small heat shock proteins and alpha-crystallins: dynamic
473 proteins with flexible functions. Trends in biochemical sciences. 2012;37(3):106-17.
474 26. Carver JA, Rekas A, Thorn DC, Wilson MR. Small heat-shock proteins and clusterin: intra-
475 and extracellular molecular chaperones with a common mechanism of action and function?
476 IUBMB life. 2003;55(12):661-8.
477 27. Haslbeck M, Buchner J. Chaperone function of sHsps. Progress in molecular and
478 subcellular biology. 2002;28:37-59.
479 28. Inoue R, Takata T, Fujii N, Ishii K, Uchiyama S, Sato N, et al. New insight into the
480 dynamical system of alphaB-crystallin oligomers. Scientific reports. 2016;6:29208.
481 29. Doss EW, Ward KA, Koretz JF. Preliminary studies on the aggregation process of alpha-
482 crystallin. Experimental eye research. 1997;65(2):255-66.
483 30. Narayan P, Meehan S, Carver JA, Wilson MR, Dobson CM, Klenerman D. Amyloid-beta
484 oligomers are sequestered by both intracellular and extracellular chaperones. Biochemistry.
485 2012;51(46):9270-6.

486 31. Cheon M, Chang I, Mohanty S, Luheshi LM, Dobson CM, Vendruscolo M, et al. Structural
487 reorganisation and potential toxicity of oligomeric species formed during the assembly of
488 amyloid fibrils. PLoS computational biology. 2007;3(9):1727-38.
489 32. Kunz C, Lonnerdal B. Human-milk proteins: analysis of casein and casein subunits by
490 anion-exchange chromatography, gel electrophoresis, and specific staining methods. The
491 American journal of clinical nutrition. 1990;51(1):37-46.
492 33. McMahon DJ, Oommen BS. Supramolecular structure of the casein micelle. Journal of
493 dairy science. 2008;91(5):1709-21.
494 34. Redwan EM, Xue B, Almehdar HA, Uversky VN. Disorder in milk proteins: caseins,
495 intrinsically disordered colloids. Current protein & peptide science. 2015;16(3):228-42.
496 35. Morgan PE, Treweek TM, Lindner RA, Price WE, Carver JA. Casein proteins as molecular
497 chaperones. Journal of agricultural and food chemistry. 2005;53(7):2670-83.
498 36. Thorn DC, Ecroyd H, Sunde M, Poon S, Carver JA. Amyloid fibril formation by bovine milk
499 alpha s2-casein occurs under physiological conditions yet is prevented by its natural
500 counterpart, alpha s1-casein. Biochemistry. 2008;47(12):3926-36.
501 37. Thorn DC, Meehan S, Sunde M, Rekas A, Gras SL, MacPhee CE, et al. Amyloid fibril
502 formation by bovine milk kappa-casein and its inhibition by the molecular chaperones alphaS-
503 and beta-casein. Biochemistry. 2005;44(51):17027-36.
504 38. Parcellier A, Schmitt E, Brunet M, Hammann A, Solary E, Garrido C. Small heat shock
505 proteins HSP27 and alphaB-crystallin: cytoprotective and oncogenic functions. Antioxidants &
506 redox signaling. 2005;7(3-4):404-13.
507 39. Yerbury JJ, Poon S, Meehan S, Thompson B, Kumita JR, Dobson CM, et al. The
508 extracellular chaperone clusterin influences amyloid formation and toxicity by interacting with
509 prefibrillar structures. FASEB journal : official publication of the Federation of American Societies
510 for Experimental Biology. 2007;21(10):2312-22.

511 40. Lu J, Cao Q, Wang C, Zheng J, Luo F, Xie J, et al. Structure-Based Peptide Inhibitor Design
512 of Amyloid-beta Aggregation. Frontiers in molecular neuroscience. 2019;12:54.
513 41. Chafekar SM, Malda H, Merkx M, Meijer EW, Viertl D, Lashuel HA, et al. Branched KLVFF
514 tetramers strongly potentiate inhibition of beta-amyloid aggregation. Chembiochem.
515 2007;8(15):1857-64.
516 42. Su Y, Chang PT. Acidic pH promotes the formation of toxic fibrils from beta-amyloid
517 peptide. Brain research. 2001;893(1-2):287-91.
518 43. Beeg M, Stravalaci M, Romeo M, Carra AD, Cagnotto A, Rossi A, et al. Clusterin Binds to
519 Abeta1-42 Oligomers with High Affinity and Interferes with Peptide Aggregation by Inhibiting
520 Primary and Secondary Nucleation. The Journal of biological chemistry. 2016;291(13):6958-66.
521 44. Bettens K, Vermeulen S, Van Cauwenberghe C, Heeman B, Asselbergh B, Robberecht C,
522 et al. Reduced secreted clusterin as a mechanism for Alzheimer-associated CLU mutations.
523 Molecular neurodegeneration. 2015;10:30.
524 45. de Retana SF, Marazuela P, Sole M, Colell G, Bonaterra A, Sanchez-Quesada JL, et al.
525 Peripheral administration of human recombinant ApoJ/clusterin modulates brain beta-amyloid
526 levels in APP23 mice. Alzheimer's research & therapy. 2019;11(1):42.
527 46. Wu L, Rosa-Neto P, Hsiung GY, Sadovnick AD, Masellis M, Black SE, et al. Early-onset
528 familial Alzheimer's disease (EOFAD). The Canadian journal of neurological sciences Le journal
529 canadien des sciences neurologiques. 2012;39(4):436-45.
530 47. LaFerla FM, Green KN. Animal models of Alzheimer disease. Cold Spring Harbor
531 perspectives in medicine. 2012;2(11).
532 48. Connelly S, Choi S, Johnson SM, Kelly JW, Wilson IA. Structure-based design of kinetic
533 stabilizers that ameliorate the transthyretin amyloidoses. Current opinion in structural biology.
534 2010;20(1):54-62.

535 49. Carrotta R, Canale C, Diaspro A, Trapani A, Biagio PL, Bulone D. Inhibiting effect of
536 alpha(s1)-casein on Abeta(1-40) fibrillogenesis. Biochimica et biophysica acta. 2012;1820(2):124-
537 32.
538 50. Raman B, Ban T, Sakai M, Pasta SY, Ramakrishna T, Naiki H, et al. AlphaB-crystallin, a
539 small heat-shock protein, prevents the amyloid fibril growth of an amyloid beta-peptide and
540 beta2-microglobulin. The Biochemical journal. 2005;392(Pt 3):573-81.
541 51. Jackson MP, Hewitt EW. Why are Functional Amyloids Non-Toxic in Humans?
542 Biomolecules. 2017;7(4).
543 52. CrysAlis^{PRO}. Agilent Technologies. Version 1.171.37.31 ed. Oxford, UK: Agilent
544 Technologies UK Ltd; 2014. p. Software system.
545 53. Battye TG, Kontogiannis L, Johnson O, Powell HR, Leslie AG. iMOSFLM: a new graphical
546 interface for diffraction-image processing with MOSFLM. Acta crystallographica Section D,
547 Biological crystallography. 2011;67(Pt 4):271-81.
548 54. Savitzky A, Golay MJE. Smoothing and Differentiation of Data by Simplified Least
549 Squares Procedures. Analytical Chemistry. 1964;36(8):1627-39.

550

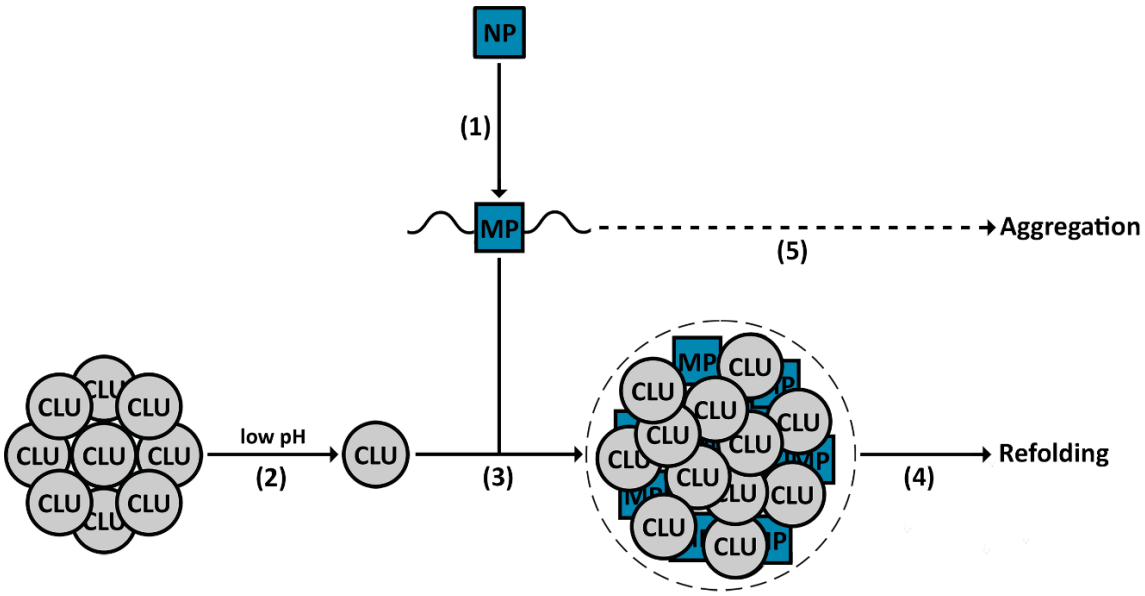

551

552 Figure 1. Representation of clusterin's molecular chaperone activity. (1) Under stress, native proteins (NP) may
553 partially unfold and become misfolded. (2) At slightly acidic pH, clusterin's (CLU) oligomers start disassociating and
554 the chaperone-active clusterin subunits get released. (3) The free clusterin subunits bind the misfolded proteins (MP)
555 and form a complex, effectively stabilizing them, (4) while other molecular chaperones refold them to their native
556 state. (5) If this mechanism proves ineffective, the misfolded proteins may form aggregates.

557

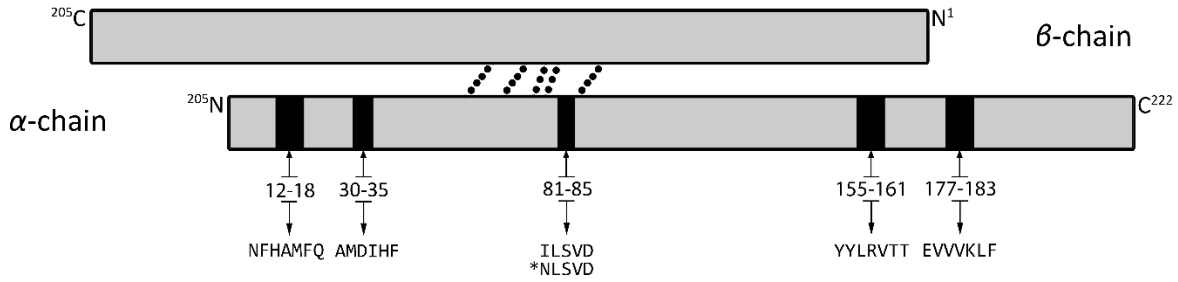

Figure 2. A simple representation of clusterin's two chains. Each chain is colored grey, with a black outline, and its sequence is numbered as found in the mature protein. The α-chain consists of 222 amino acid residues. The β-chain is slightly shorter, consisting of 205 amino acid residues. The two chains are joined by five disulfide bonds, depicted as black dots. The aggregation-prone regions of the α-chain are depicted as black rectangles on clusterin's sequence.

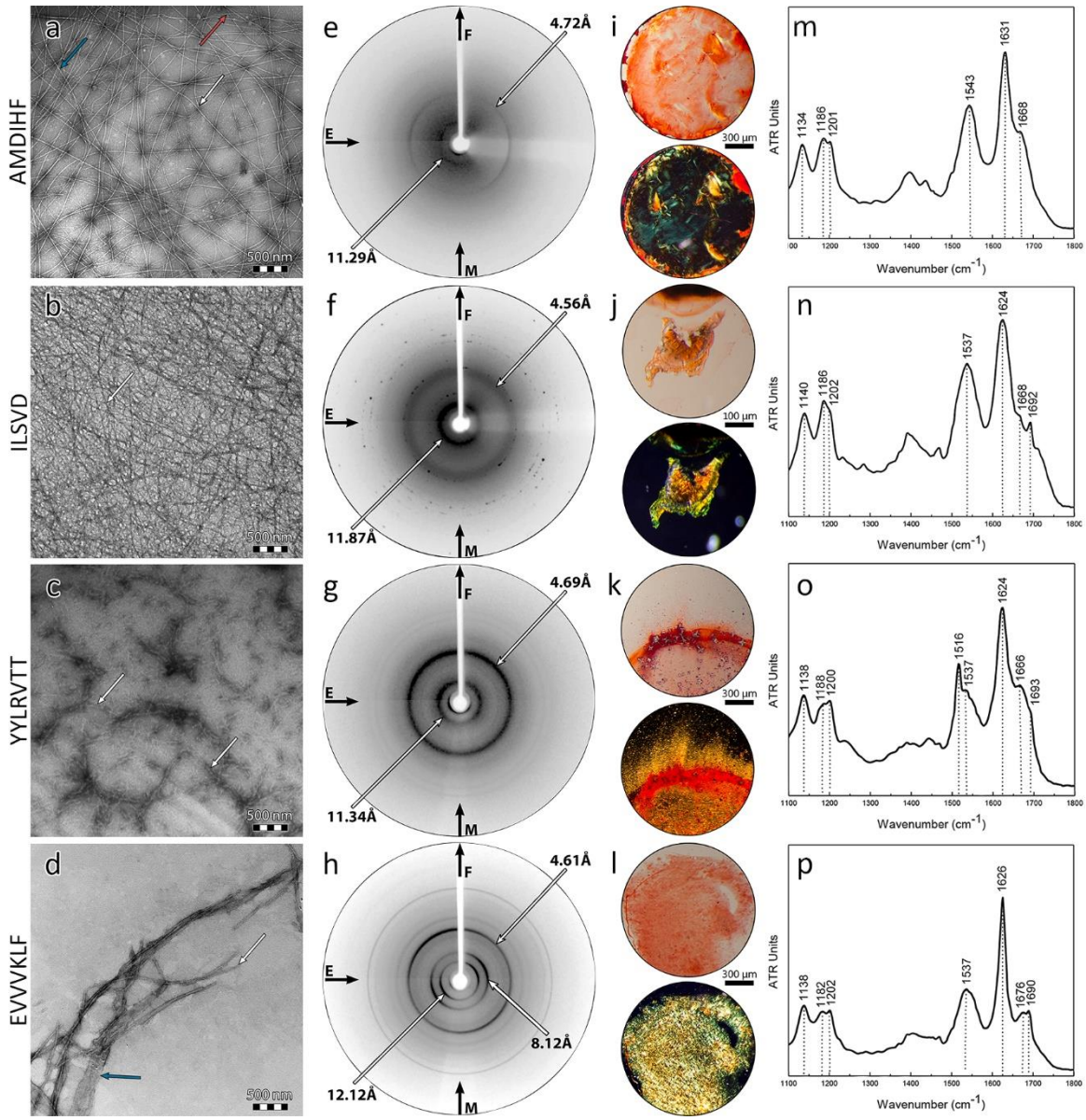

Figure 3. All the peptide-analogues fulfill the experimental criteria. (a-d) Transmission electron micrographs of amyloid-like fibrils derived from self-assemblies of peptides AMDIHF, ILSVD, YYLRVTT and EVVVKLF at 500 µM, respectively. The white arrows mark single fibrils with the diameter of typical amyloid fibrils, the red arrow marks a supercoil and the blue arrows mark tapes. (e-h) X-ray diffraction patterns of oriented fibers, derived from the four peptides at 1 mM, respectively. Reflections marked with arrows are indicative of the "cross-*β*" structure, which amyloids typically have. (i-l) Photomicrographs of gels, derived from self-assemblies of the four peptides at 500 µM, respectively. The Congo red dye is bound, as seen under bright field illumination (upper). The apple-green birefringence that amyloids typically exhibit is observed under crossed polars (lower). (m-p) ATR FT-IR spectra (1100–1800 cm^{-1}) produced from thin hydrated films created by solutions of the four peptides at 500 µM, respectively. Fibrils derived from each peptide has *β*-sheet secondary structure, as hinted by the presence of strong amide I and II bands.

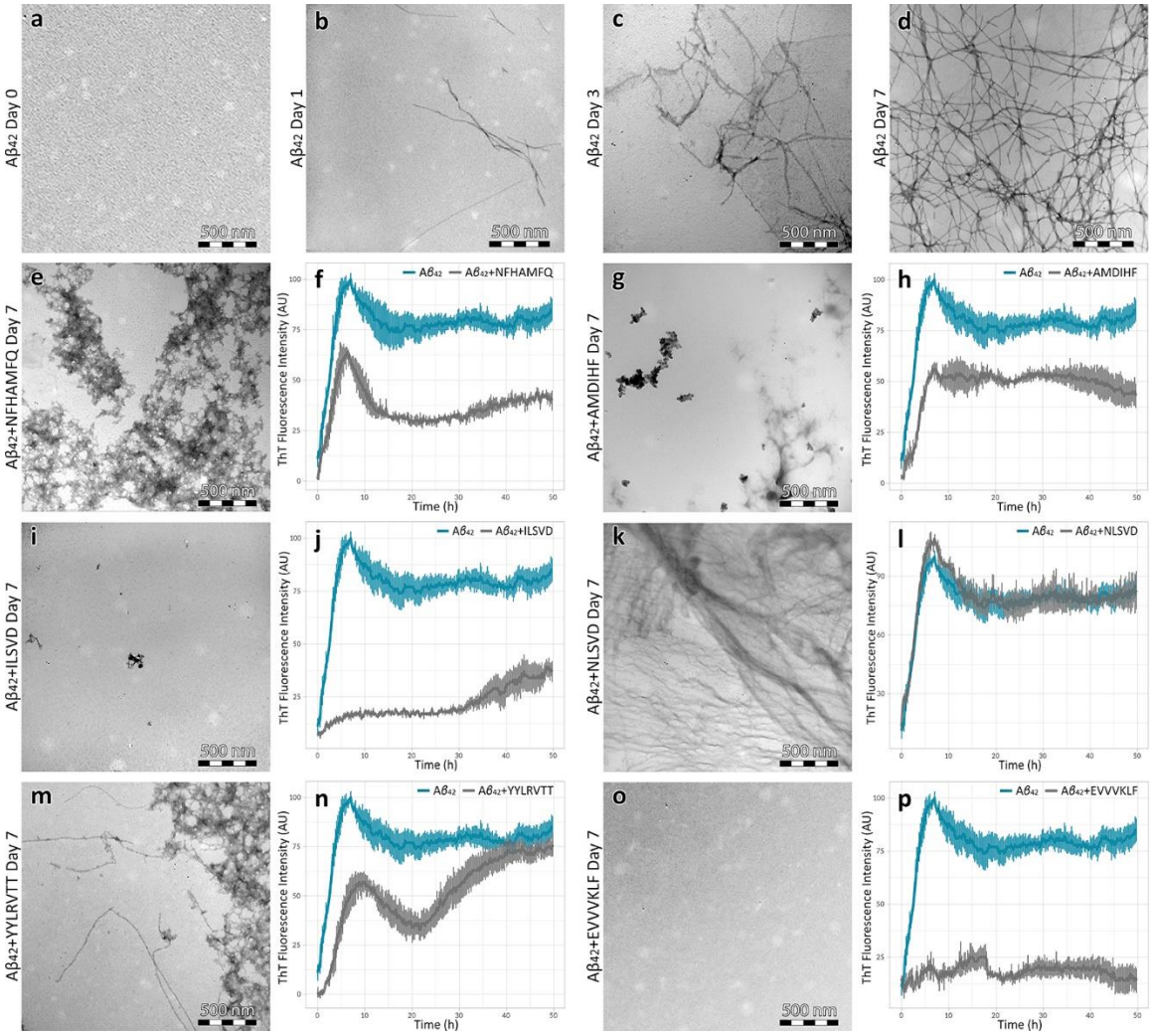

Figure 4. Clusterin peptide-analogues inhibit or delay Aβ_{42} fibril formation. (a-d) Transmission electron micrographs of Aβ_{42}, incubated for 0, 1, 3 and 7 days, respectively. Amyloid fibrils are observed from day 1 to day 7. The number of fibrils raises as incubation time increases. (e, f) Transmission electron micrograph and Thioflavin T fluorescence emission spectrum of Aβ_{42} co-incubated with NFHAMFQ for 7 days and over a period of 50 hours, respectively. (g, h) Transmission electron micrograph and Thioflavin T fluorescence emission spectrum of Aβ_{42} co-incubated with AMDIHF for 7 days and over a period of 50 hours, respectively. (i, j) Transmission electron micrograph and Thioflavin T fluorescence emission spectrum of Aβ_{42} co-incubated with ILSVD for 7 days and over a period of 50 hours, respectively. (k, l) Transmission electron micrograph and Thioflavin T fluorescence emission spectrum of Aβ_{42} co-incubated with the mutant peptide, NLSVD, for 7 days and over a period of 50 hours, respectively. (m, n) Transmission electron micrograph and Thioflavin T fluorescence emission spectrum of Aβ_{42} co-incubated with YYLRVTT for 7 days and over a period of 50 hours, respectively. (o, p) Transmission electron micrograph and Thioflavin T fluorescence emission spectrum of Aβ_{42} co-incubated with EVVVKLF for 7 days and over a period of 50 hours, respectively. Error bars in ThT fluorescence emission spectra represent standard deviation among triplicates. 100 µM solutions were used for TEM, while 10 mM solutions were used for the ThT kinetics assays.

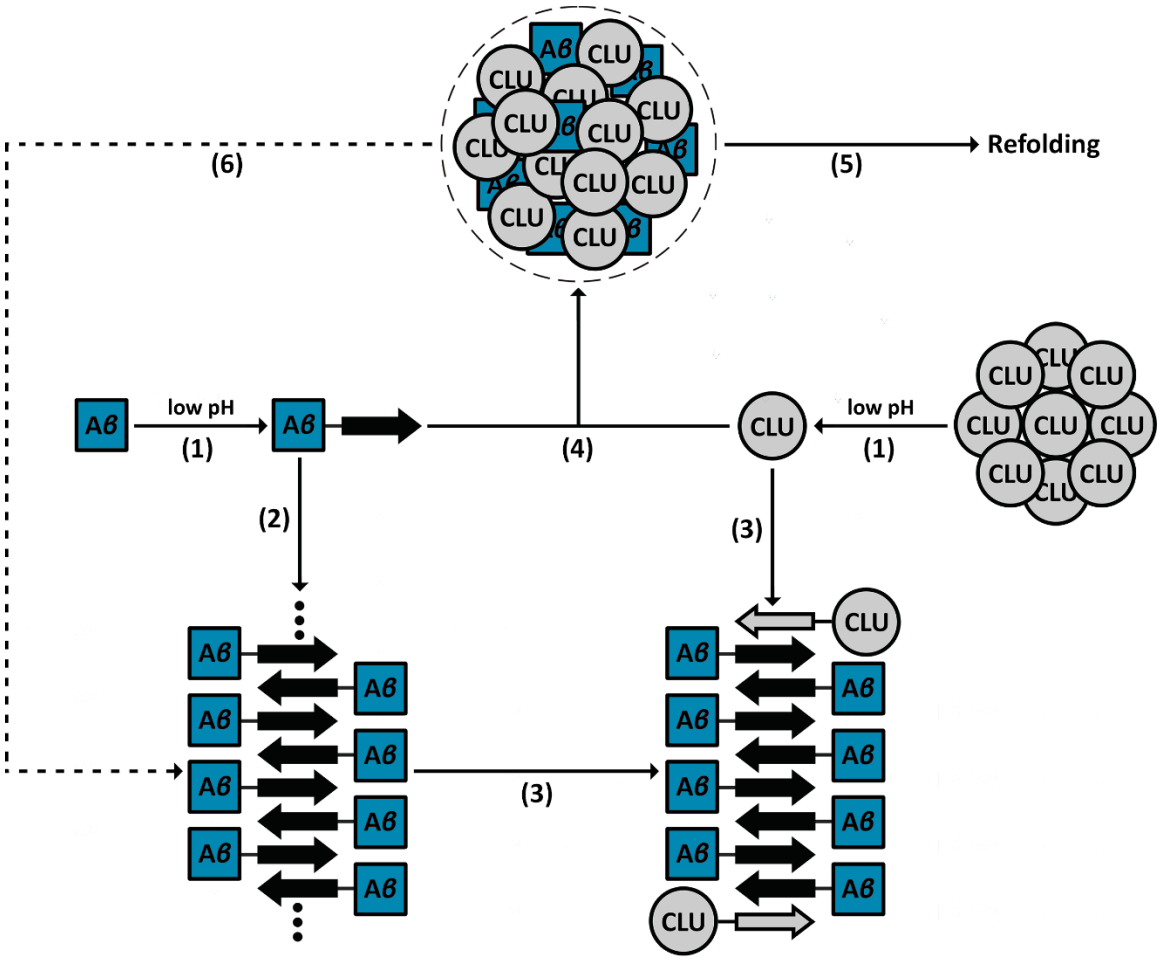

591

592 Figure 5. Putative mechanism of clusterin-mediated inhibition of A*β* amyloidogenesis. (1) Under acidic pH-induced
593 stress, A*β* may partially unfold, exposing hydrophobic regions with the propensity to form *β*-strands. At the same
594 time, the acidic pH triggers the disassociation of clusterin's heterogeneous aggregates. (2) Misfolded A*β* begin to
595 form amyloid fibrils, but (3) the disassociated clusterin subunits (CLU) halt fibril growth, utilizing their aggregation-
596 prone regions, which tend to form *β*-strands as well. (4) Clusterin binds misfolded A*β* monomers, forming complexes
597 and stabilizes their structure, until (5) they are refolded by other molecular chaperones. (6) In case misfolded A*β*
598 species are produced faster than clusterin can stabilize their structure, it essentially brings them into proximity with
599 remote monomers, accelerating amyloid formation.

600

601 Table 1. Bands observed in the ATR FT-IR spectra obtained from thin hydrated films produced by AMDIHF, EVVVKLF,
602 YYLRVTT and ILSVD solutions, respectively, and their tentative assignments.

AMDIHF bands	ILSVD bands	YYLRVTT bands	EVVVKLF bands	Band assignments
1134	1140	1138	1138	TFA
1186	1186	1188	1182	TFA
1201	1202	1200	1202	TFA
-	-	1516	-	Tyrosine
1543	1537	1537	1537	*β*-sheet
1631	1624	1624	1626	*β*-sheet
1668	1668	1666	1676	TFA
-	1692	1693	1690	Antiparallel *β*-sheet

603